Decreased body weight and hepatic steatosis with altered fatty acid ethanolamide metabolism in aged *L-Fabp*$^{-/-}$ mice[S]

Elizabeth P. Newberry,* Susan M. Kennedy,* Yan Xie,* Jianyang Luo,* Rosanne M. Crooke,† Mark J. Graham,† Jin Fu,§ Daniele Piomelli,§, and Nicholas O. Davidson[1],***

Department of Medicine,* Washington University School of Medicine, St. Louis, MO; Isis Pharmaceuticals Inc.,† Carlsbad, CA; Department of Pharmacology,§ University of California, Irvine, CA; and Drug Discovery and Development,** Italian Institute of Technology, Genoa, Italy

Abstract **The tissue-specific sources and regulated production of physiological signals that modulate food intake are incompletely understood. Previous work showed that *L-Fabp*$^{-/-}$ mice are protected against obesity and hepatic steatosis induced by a high-fat diet, findings at odds with an apparent obesity phenotype in a distinct line of aged *L-Fabp*$^{-/-}$ mice. Here we show that the lean phenotype in *L-Fabp*$^{-/-}$ mice is recapitulated in aged, chow-fed mice and correlates with alterations in hepatic, but not intestinal, fatty acid amide metabolism. *L-Fabp*$^{-/-}$ mice exhibited short-term changes in feeding behavior with decreased food intake, which was associated with reduced abundance of key signaling fatty acid ethanolamides, including oleoylethanolamide (OEA, an agonist of PPARα) and anandamide (AEA, an agonist of cannabinoid receptors), in the liver. These reductions were associated with increased expression and activity of hepatic fatty acid amide hydrolase-1, the enzyme that degrades both OEA and AEA. Moreover, *L-Fabp*$^{-/-}$ mice demonstrated attenuated responses to OEA administration, which was completely reversed with an enhanced response after administration of a nonhydrolyzable OEA analog. These findings demonstrate a role for L-Fabp in attenuating obesity and hepatic steatosis, and they suggest that hepatic fatty acid amide metabolism is altered in *L-Fabp*$^{-/-}$ mice.**—Newberry, E. P., S. M. Kennedy, Y. Xie, J. Luo, R. M. Crooke, M. J. Graham, J. Fu, D. Piomelli, and N. O. Davidson. **Decreased body weight and hepatic steatosis with altered fatty acid ethanolamide metabolism in aged *L-Fabp*$^{-/-}$ mice. *J. Lipid Res.* 2012.** 53: **744–754.**

Supplementary key words fatty acid binding protein • satiety • obesity • feeding behavior

The prevalence of nonalcoholic fatty liver disease, type II diabetes, and the metabolic syndrome has increased dramatically in the past 20 years, in parallel with the epidemic of obesity. Although environmental factors (caloric excess) and lifestyle choices (lack of exercise) are the primary causes, genetic susceptibility also predisposes individuals to obesity and its metabolic complications. Studies have identified mechanisms by which food consumption is regulated, including release of factors produced within the gastrointestinal tract (CCK, ghrelin, PYY, lipid amides, and palmitoleic acid) that mediate satiety either locally or centrally (1).

Recent studies have identified several lipid messengers that regulate feeding behavior (2–5). These include the endocannabinoids, anandamide (AEA) and 2-arachidonoylglycerol (endogenous ligands of the cannabinoid receptors); the fatty acid ethanolamides (FAE), oleoylethanolamide (OEA) and palmitoylethanolamide (PEA); and their biosynthetic precursors, the *N*-acyl-phosphatidylethanolamines (6, 7). OEA is an ubiquitous lipid molecule that is synthesized in the proximal small intestine following consumption of dietary fat, and it promotes satiety by binding nuclear peroxisome proliferator-activated receptor-α (PPARα) and activating vagal efferents (8–10). Conversely, AEA promotes food consumption through activation of CB_1 cannabinoid receptors both in the brain and peripheral tissues. In addition, AEA regulates systemic energy utilization, inflammation, apoptosis, and pain (11, 12). Details of how the balance between opposing satiety and orexigenic factors is maintained are a focus of investigation, but there is increasing evidence for a role of intracellular

This work was supported by National Institutes of Health Grants DK-56260 (N.O.D.), DK-52574 (N.O.D.), HL-38180 (N.O.D.), and DK-073955 (D.P.). Its contents are solely the responsibility of the authors and do not necessarily represent the official views of the National Institutes of Health.

Manuscript received 27 September 2011 and in revised form 6 February 2012.

Published, JLR Papers in Press, February 8, 2012
DOI 10.1194/jlr.M020966

Abbreviations: AEA, anandamide; ASO, antisense oligonucleotide; FAAH, fatty acid amide hydrolase; FABP, fatty acid binding protein; FAE, fatty acid ethanolamide; OEA, oleoylethanolamide; PEA, palmitoylethanolamide; PL, phospholipid; PPARα, peroxisome proliferator-activated receptor α; QTL, quantitative trait loci; SF, saturated fat; SSLP, simple sequence length polymorphism; TG, triglyceride; WT, wild-type.

[1]To whom correspondence should be addressed.
e-mail: NOD@WUSTL.EDU

[S] The online version of this article (available at http://www.jlr.org) contains supplementary data in the form of two tables.

carrier proteins, including fatty acid binding proteins (FABP), in the metabolic compartmentalization of these mediators (13, 14).

L-Fabp is an abundant cytosolic FABP expressed in hepatocytes and in enterocytes of the proximal small intestine. Our studies have demonstrated that female mice with germline deletion of *L-Fabp* are protected against weight gain and hepatic steatosis when fed high saturated fat (SF) diets (15–17). This phenotype cannot be attributed to increased energy metabolism or decreased absorption of dietary fat, although the kinetics of intestinal fatty acid (FA) uptake is altered in *L-Fabp*$^{-/-}$ mice (17, 18). In general, *L-Fabp*$^{-/-}$ mice fed a high-fat diet exhibit a subtle (although not statistically significant) decrease in average daily food consumption, a difference which would over time be sufficient to reduce weight gain (15).

However, understanding the role of *L-Fabp* in attenuating obesity and hepatic steatosis in the setting of high-fat feeding has been complicated by the phenotype of a distinct line of *L-Fabp*$^{-/-}$ mice that exhibits markedly increased adiposity in aged (9- to 18-month-old) mice fed a chow diet (19). Acknowledging that our previous characterizations were undertaken in mice less than 24 weeks of age fed a high-fat diet, we entertained the possibility that an obesity phenotype in chow-fed mice might only become apparent in aged *L-Fabp*$^{-/-}$ animals. We also investigated the potential role of genetic background in mediating the divergent phenotypes, using liver specific knockdown of *L-Fabp* in two inbred mouse strains. Finally, we investigated some potential mechanisms by which deletion of *L-Fabp* may affect the susceptibility to obesity and hepatic steatosis by examining feeding behavior and the metabolism and signaling of orexigenic and anorectic factors.

METHODS

Animals

C57BL/6J congenic *L-Fabp*$^{-/-}$ mice were generated in our lab and backcrossed using a speed congenic strategy (16). C57BL/6J and 129/SvJ mice (controls and the antisense oligonucleotides [ASO] studies) were obtained from Jackson Laboratory (Bar Harbor, ME). *Ob/Ob* (C57BL/6J congenic, Jackson Laboratory) mice were bred with *L-Fabp*$^{-/-}$ mice to produce double knockouts. Unless otherwise noted, female mice were used for all experiments, and mice were maintained on a 12 h light/dark cycle and fed standard rodent chow. High-SF diet (#960242, MP Biomedical, Santa Ana, CA) and Western diet (#88137, Harlan Teklad, Madison, WI) feeding studies were initiated at 8–10 weeks of age. ASO were designed and synthesized by Isis Pharmaceuticals (Carlsbad, CA). ASOs were injected biweekly (50 mg/kg ip) for 6–8 weeks, either concurrent with or ~6 weeks after start of high-fat diet feeding. Two distinct *L-Fabp* ASOs produced similar knockdown of hepatic *L-Fabp* expression (determined by Q-PCR) and resultant phenotype, with no change in intestinal *L-Fabp* expression. All animal protocols followed National Institutes of Health guidelines and were approved by the Washington University Animal Studies Committee.

In vivo analyses

Dietary cholesterol absorption was determined as described (20). Magnetic resonance imaging (MRI) analyses were performed on 1-year-old mice using an EchoMRI 3in1 (Echo Medical Systems, Houston, TX). Hepatic VLDL production was determined following a 4 h fast as described (21) using Pluronic F127 (1 g/kg iv, Invitrogen, Camarillo, CA). Blood was collected and serum triglyceride (TG) measured prior to injection of Pluronic F127 and at 30 min intervals thereafter. For acute feeding studies, mice were housed individually on metabolic racks for over 7 days prior to the start of the experiment, fasted 24 h starting at 10:00 h, with food consumption measured 2–6 h after refeeding. In some experiments, mice were injected intraperitoneally with OEA (10 mg/kg, Calbiochem, Rockland, MA), methyl-OEA (10 mg/kg) synthesized as described (22), or vehicle (5% Tween-80, 5% propylene glycol in saline) 1 h prior to refeeding, with food consumption measured at 2 h and compared with baseline food consumption (vehicle/uninjected) examined at least one week prior to experiments with OEA.

In vitro studies

RNA was isolated (Trizol, Invitrogen) and cDNA was prepared as described (16). Real time PCR was performed on Step One Plus (ABI) using Fast SYBR Green Master Mix (ABI) as described (16). Primer sequences are listed in supplementary Table I. FAAH activity was measured as described (8) using membranes prepared from frozen liver tissue. FAE levels were measured in liver, jejunal mucosa, and serum of fasted (24 h starting at 18:00 h) or free-fed, chow-diet mice that were sacrificed at start of dark cycle (18:00 h) as described (8). OEA and other fatty acid ethanolamides were quantified after lipid extraction by isotope-dilution liquid chromatography/mass spectrometry as previously detailed (8). Kits for measurement of TG, cholesterol, free fatty acids (FFA), and phospholipids (PL) were from Wako Chemicals (Richmond, VA) as described (15).

Simple sequence length polymorphism mapping

Markers that produced informative differences between C57BL/6J and 129/SvJ mice are listed in supplementary Table II. PCR products (36 cycles of 94°C, 30 s; 56°C, 45 s; 72°C, 45 s) were separated on a 4% SFR Agarose gel (Midwest Scientific, St Louis, MO) in TBE buffer, with C57BL/6J and 129/SvJ controls run alongside.

Statistical analyses

Statistical comparisons were performed using Student *t*-test (two tailed, unpaired) in Microsoft Excel or GraphPad Prism (San Diego, CA). Data are shown as mean ± SE unless otherwise noted.

RESULTS

Aged female *L-Fabp*$^{-/-}$ mice are protected against weight gain and hepatic steatosis

Our earlier studies demonstrated that female *L-Fabp*$^{-/-}$ mice are protected against obesity and hepatic steatosis induced by a high-SF diet (15, 17). However, in view of the divergent (i.e., obesity-prone) phenotype observed in aged, chow-fed *L-Fabp*$^{-/-}$ mice generated from another laboratory (19), we considered the possibility that an obesity phenotype in chow-fed *L-Fabp*$^{-/-}$ mice might only become apparent upon aging. However, this turned out not to be the case. In contrast to those studies (19), our chow-diet–fed female *L-Fabp*$^{-/-}$ mice weighed significantly less than C57BL/6J control wild-type (WT) mice (**Fig. 1A**) after 5 months of age, with decreased fat mass as determined by both MRI (Fig. 1B) and DEXA (data not shown) analysis at

12 months. Mice were sacrificed at 13 months for analysis of serum and tissue lipid levels (**Table 1**). Hepatic TG content (Fig. 1C) and VLDL secretion (Fig. 1D) were both reduced in *L-Fabp*$^{-/-}$ mice, with no difference in hepatic cholesterol, PL, or FFA content (Table 1). There was no change in the absorption efficiency of dietary fat [data not shown, consistent with our prior observations (15, 17)], but intestinal cholesterol absorption was reduced in aged *L-Fabp*$^{-/-}$ mice (Fig. 1E), as observed previously in younger *L-Fabp*$^{-/-}$ mice (20). We also examined the possibility that fatty acid oxidation might be upregulated as a mechanism to account for the attenuated weight gain and hepatic steatosis. The findings revealed reduced mRNA abundance of several candidate genes involved in fatty acid oxidation, including PPARα and several PPARα target genes (Cpt1L, Acadl, and Acadm), in livers of *L-Fabp*$^{-/-}$ mice (Fig. 1F), making it unlikely that increased fatty acid oxidation accounts for the phenotype in these animals. Thus, *L-Fabp*$^{-/-}$ mice fed a low-fat chow diet exhibit an age-dependent reduction in body weight and hepatic TG accumulation, a phenotype that recapitulates our earlier observations in *L-Fabp*$^{-/-}$ mice fed a high-SF diet (15, 17).

We next examined whether *L-Fabp*$^{-/-}$ mice might exhibit increased adiposity on a chow diet in the setting of leptin deficiency and hyperphagia. *L-Fabp*$^{-/-}$ *Ob/Ob* mice displayed an initial trend toward decreased body weight compared with *Ob/Ob* controls (3–9 weeks of age, **Fig. 2**), but this difference disappeared by 20 weeks of age. In line with the observations above, chow-fed female *L-Fabp*$^{-/-}$ *Ob/+* mice weighed less than *Ob/+* mice after ~16 weeks of age (Fig. 2). As expected, both *Ob/Ob* and *L-Fabp*$^{-/-}$ *Ob/Ob* mice were hyperphagic compared with *Ob/+* controls, but there was no detectable difference between the genotypes (data not shown). Serum and hepatic lipid content and liver and fat mass did not differ between the *Ob/Ob* genotypes (not shown). These data suggest that hyperphagia abrogates the reductions in body weight observed in leptin-sufficient female *L-Fabp*$^{-/-}$ mice, implying that changes in food consumption may contribute to the phenotype of *L-Fabp*$^{-/-}$ mice.

Analysis of quantitative trait loci related to body weight near *Fabp1* locus reveals no evidence of gene duplication

The murine *Fabp1* gene is located in a chromosomal region containing numerous quantitative trait loci (QTL) and genes related to body weight and obesity (**Fig. 3A**). Simple sequence length polymorphism (SSLP) marker analysis showed that the C57BL/6J congenic *L-Fabp*$^{-/-}$ mice used in these studies contain at most 17 cM of 129/SvJ genomic DNA [originating from the ES cell line (16)] around the *Fabp1* locus (Fig. 3A). Although this is a relatively small amount of non-C57BL/6J genomic DNA, several obesity-related QTLs are located within this region. To address the possibility that the obesity-protection phenotype in *L-Fabp*$^{-/-}$ mice might reflect altered expression of a nearby modifier gene (i.e., allelic variation or gene duplication), we surveyed the expression of structural genes located near *Fabp1* in the livers of female C57BL/6J and *L-Fabp*$^{-/-}$ mice (Fig. 3B). There was a subtle (~35%) increase in the expression of 2 out of 11 genes (Fkbp9 and Abcg2) in young *L-Fabp*$^{-/-}$ mice compared with young C57BL/6J mice (**Table 2**), although these differences were not recapitulated in the liver of aged *L-Fabp*$^{-/-}$ mice or in intestinal mucosa (data not shown), and Western blotting revealed no changes in protein abundance (data not shown). We also verified that there was no residual expression of L-Fabp mRNA either from the targeted exons (exons 1 and 2) or from downstream exons (exons 3/4), thereby eliminating the concern that our targeting strategy might have produced a hypomorphic allele (Table 2). Together these data indicate that expression of genes located near *Fabp1* locus is not dramatically altered in *L-Fabp*$^{-/-}$ mice, making it unlikely that polymorphic alterations in a modifier gene contribute to the phenotype observed.

Protection against and reversal of high SF diet-induced obesity and hepatic steatosis with liver-specific L-Fabp knockdown in distinct genetic backgrounds

As an independent strategy to explore the potential influence of genetic background on the obesity-protection phenotype resulting from *L-Fabp* deletion, we injected female C57BL/6J and 129/SvJ inbred mice with antisense oligonucleotides to decrease hepatic L-Fabp expression. ASO-mediated knockdown reduced hepatic L-Fabp expression by ~70% (data not shown) without producing changes in intestinal L-Fabp expression, similar to our previous observations (23). ASO injections initiated concomitant with Western diet feeding significantly reduced weight gain and hepatic steatosis in both C57BL/6J (**Fig. 4A**) and 129/SvJ mice (Fig. 4B) compared with control ASO-injected mice. These findings imply that liver-specific knockdown of L-Fabp phenocopies the effects of germline *L-Fabp* deletion. Moreover, treatment with L-Fabp ASO reversed obesity and hepatic steatosis in mice fed a SF diet for six weeks prior to starting ASO injections (Fig. 4C, D), with L-Fabp ASO abrogating weight gain after the first week of ASO injections. As above, this effect was observed in both C57BL/6J (Fig. 4C) and 129/SvJ (Fig. 4D) mice, suggesting that the phenotype noted with germline *L-Fabp* deletion is unlikely to be due to strain effects from residual 129/SvJ gDNA near the targeted locus. C57BL/6J mice treated with L-Fabp ASO exhibit reduced food consumption (Fig. 4E), a decrease similar to the trend observed previously in *L-Fabp*$^{-/-}$ mice fed a high-SF diet (17). Treatment with L-Fabp ASO did not alter dietary fat absorption (control ASO, 98.8 ± 0.07% absorbed; L-Fabp ASO, 98.9 ± 0.08%, n = 6–8, C57BL/6J cohort) or expression of genes involved in hepatic fatty acid oxidation (Fig. 4G). Together these data demonstrate that knockdown of hepatic L-Fabp expression reduces diet-induced obesity and hepatic steatosis in both C57BL/6J and 129/SvJ backgrounds. The findings also suggest that alterations in food consumption may be associated with this phenotype.

Potential explanations for decreased body weight in aged *L-Fabp*$^{-/-}$ mice

Although the deletion of *L-Fabp*, either systemically or only in the liver, markedly affects body weight, the mechanism for

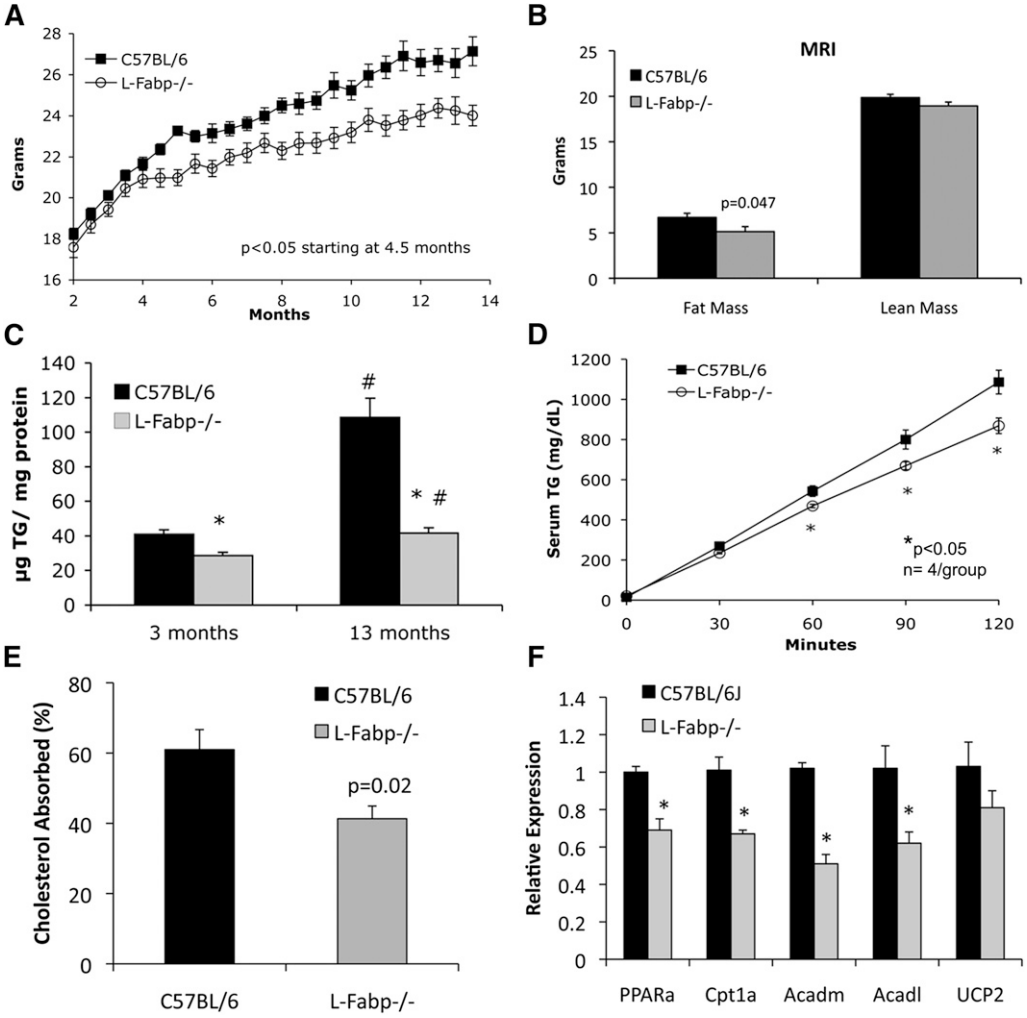

Fig. 1. Aged chow-fed *L-Fabp*$^{-/-}$ mice exhibit reduced body weight and hepatic steatosis. A: Average body weight of aged chow-fed mice. n = 10–11 animals/group. B: Determination of lean and fat mass using magnetic resonance imaging (MRI) in 1-year-old female mice. n = 10–11 animals/group. C: Hepatic TG content of young (3-month-old) and aged (13-month-old) mice. *$P < 0.01$ versus WT mice of same age. $^{\#}P < 0.01$ in young versus old mice of the same genotype. n = 5–7 mice/group. D: Hepatic VLDL production in aged chow-fed mice. E: Dietary cholesterol absorption in aged chow-fed mice. n = 5 mice/group. F: Relative expression of genes involved in fatty acid oxidation in livers of aged chow-fed mice. n = 4 C57BL/6J mice and 5 *L-Fabp*$^{-/-}$ mice.

this phenotype remains unclear. As mentioned above, *L-Fabp* deletion does not affect the overall efficiency of dietary fat absorption. In addition, utilization of FA through oxidation is either unchanged (ASO, Fig. 4G) or decreased (*L-Fabp*$^{-/-}$, Fig. 1F), based on hepatic expression of FAO genes. In previous studies, we found that *L-Fabp*$^{-/-}$ mice fed high-SF diets exhibit a subtle but consistent trend of decreased food consumption (<0.2 g/day, nonsignificant) (20). Despite the small magnitude of this difference, energy balance calculations showed that a minor decrease in energy intake would ultimately be sufficient to lead to the observed differences in weight gain. In the current studies, however, we observed no difference in average daily food consumption between chow-fed C57BL/6J and *L-Fabp*$^{-/-}$ female mice, at either 6 months of age (WT, 3.72 ± 0.05 g/day; *L-Fabp*$^{-/-}$, 3.84 ± 0.13 g/day, n = 6–8, $P = 0.47$) or 13 months (Table 1) of age. It is worth suggesting that average daily food intake data should be interpreted with caution, as other authors have pointed out the intrinsic difficulties in discerning small (i.e., ±10%) but real differences in food consumption (24). Accordingly, we examined the possibility that *L-Fabp* deletion may induce a subtle change in acute feeding behavior (i.e., food consumed per meal, meal latency) that in turn might lead to reduced body weight, a possibility supported by other work (25) along with our previous finding that respiratory exchange ratio (17) was chronically elevated in *L-Fabp*$^{-/-}$ mice fed a Western diet (suggesting a shift in energy substrate utilization from fat to carbohydrate). We therefore examined short-term feeding responses following a 24 h fast and found that chow-fed *L-Fabp*$^{-/-}$ mice consumed ~0.2 g less than WT mice ($P < 0.02$) in the 6 h after refeeding (**Fig. 5A**), a difference that persisted even after correcting for differences in body weight (Fig. 5B). A similar difference in acute food consumption was observed in mice fed a SF diet for six weeks prior to the experiment (Fig. 5C), although the differences

TABLE 1. Physiological parameters in aged (13-month-old) female mice

	C57BL/6 Female Mice	*L-Fabp*$^{2/2}$ Female Mice	*P*
Body weight (g)	26.6 ± 0.7 (10)	23.9 ± 0.7 (9)	0.013
Liver weight (g)	1.2 ± 0.04 (10)	1.1 ± 0.04 (9)	NS
Liver/body (%)	4.6 ± 0.1 (10)	4.6 ± 0.1 (9)	NS
Fat (g)	0.8 ± 0.1 (10)	0.5 ± 0.1 (9)	0.053
Fat/body (%)	2.8 ± 0.3 (10)	2.0 ± 0.2 (9)	NS
Serum TG (mg/dl)	33.6 ± 2.9 (10)	35.0 ± 3.8 (9)	NS
Serum cholesterol (mg/dl)	45.6 ± 1.5 (10)	44.4 ± 1.3 (9)	NS
Serum FFA (mmol/l)	0.501 ± 0.046 (10)	0.463 ± 0.79 (9)	NS
Serum glucose (mg/dl)	249.4 ± 18.4 (10)	248.3 ± 13.1 (9)	NS
Food consumption (g/day)	4.10 ± 0.14 (7)	4.29 ± 0.11 (8)	NS
Hepatic TG (μg/mg protein)	108.4 ± 11.2 (6)	41.6 ± 3.1 (5)	0.001
Hepatic cholesterol (μg/mg protein)	25.3 ± 2.2 (6)	23.8 ± 0.9 (5)	NS
Hepatic FFA (nmol/mg protein)	98.5 ± 9.8 (6)	86.6 ± 4.4 (5)	NS
Hepatic PL (μg/mg protein)	85.7 ± 5.0 (6)	89.1 ± 2.5 (5)	NS

Numbers in parentheses indicate number of animals examined. NS, nonsignificant.

were abrogated when normalized to body weight, because as expected, body weight of the *L-Fabp*$^{-/-}$ cohort was significantly reduced compared with controls (Fig. 5D).

Fatty acid ethanolamide content is altered in *L-Fabp*$^{-/-}$ mice

Previous work established that the kinetics of FA uptake and trafficking are reduced in *L-Fabp*$^{-/-}$ mice (17, 18), raising the possibility that the synthesis or metabolism of lipid-derived satiety or orexigenic factors might be altered, which might lead in turn to altered feeding behavior. To address this question, we examined tissue and serum levels of the fatty acid ethanolamides OEA, PEA, and AEA. There was no difference by genotype in abundance of the satiety factor OEA in jejunal mucosa in either fasting or fed mice (**Fig. 6A**), but we found a marked decrease in hepatic levels of both OEA and PEA in fasted and fed *L-Fabp*$^{-/-}$ mice (Fig. 6B, C). In addition, serum OEA levels were decreased in fasted *L-Fabp*$^{-/-}$ mice and demonstrated a trend to decrease in fed mice (Fig. 6D). Importantly, levels of the orexigenic acyl ethanolamide AEA were significantly decreased in livers from fasted *L-Fabp*$^{-/-}$ mice, matching levels observed in fed C57BL/6 mice (Fig. 6E). These data suggest that the abundance of key mediators of satiety and acute food consumption are altered in *L-Fabp*$^{-/-}$ mice, differences which could potentially explain the subtle differences in acute feeding behavior observed in these animals, despite the absence of a discernible difference in overall food intake measured over several days.

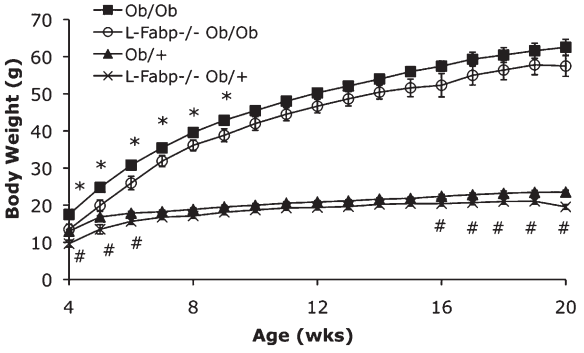

Fig. 2. Disruption of leptin signaling abrogates protection from obesity in *L-Fabp*$^{-/-}$ mice. Body weight of female *Ob/Ob*, *L-Fabp*$^{-/-}$ *Ob/Ob*, *Ob/+*, and *L-Fabp*$^{-/-}$ *Ob/+* mice from 4 to 20 weeks of age. $^{*}p < 0.05$ in *L-Fabp*$^{-/-}$ *Ob/Ob* versus *Ob/Ob* mice. $^{\#}p < 0.05$ in *L-Fabp*$^{-/-}$ *Ob/+* compared with *Ob/+* mice. n = 6–8 animals/group.

Fatty acid ethanolamide metabolism is altered in *L-Fabp*$^{-/-}$ mice

Because of the striking reduction in hepatic FAE levels in *L-Fabp*$^{-/-}$ mice (Fig. 6), we surveyed hepatic expression of genes related to FAE synthesis, degradation, and signaling, which were generally unchanged (**Fig. 7A**). Two exceptions to this observation were expression of fatty acid amide hydrolase-1 (FAAH-1), the enzyme responsible for AEA, OEA, and PEA hydrolysis, and expression of Trpv1 (Capsaicin receptor), a receptor for AEA. FAAH-1 mRNA levels were unchanged in the livers of younger mice but increased in both older, chow-fed mice and SF-fed *L-Fabp*$^{-/-}$ mice (Fig. 7B). Furthermore, FAAH enzymatic activity was significantly increased in hepatic extracts of both aged chow-fed and SF-fed *L-Fabp*$^{-/-}$ mice (Fig. 7C). Trpv1 mRNA was significantly reduced in livers of aged *L-Fabp*$^{-/-}$ mice (as noted above) and exhibited a trend to decrease in livers of younger mice (data not shown). Taken together, the data suggest that decreased FAE levels in livers of *L-Fabp*$^{-/-}$ mice may result from increased degradation via upregulation of FAAH-1. In addition, FAE signaling may be impaired due to decreased expression of Trpv1, as suggested by the demonstration that Trpv1 deletion is associated with protection against diet-induced obesity (26).

Intestinal production of the lipid messenger OEA leads to satiety, with exogenous OEA triggering a marked decrease in acute feeding (4, 5). Consistent with these findings, injection of OEA into C57BL/6J mice produced a significant decrease in food consumption 2 h after refeeding (Fig. 7D, left bars). However, this response was blunted in *L-Fabp*$^{-/-}$ mice (Fig. 7D, left bars). To investigate the possibility that the reduction in OEA-mediated satiety in *L-Fabp*$^{-/-}$ mice was due to increased FAAH-1 activity, we synthesized a nonhydrolyzable OEA analog (methyloleoylethanolamide, Meth-OEA) (22), a compound whose levels would not be influenced by alterations in FAAH activity, and studied its effects on feeding behavior. Meth-OEA produced a profound reduction in food consumption in both genotypes and eliminated the attenuated response observed in *L-Fabp*$^{-/-}$ mice when native OEA was administered (Fig. 7D, right bars). These data suggest that alterations in FAE metabolism in *L-Fabp*$^{-/-}$ mice, including increased hydrolysis of FAE, may lead to increased satiety and altered acute food consumption, which we propose may contribute to attenuated weight gain in these animals.

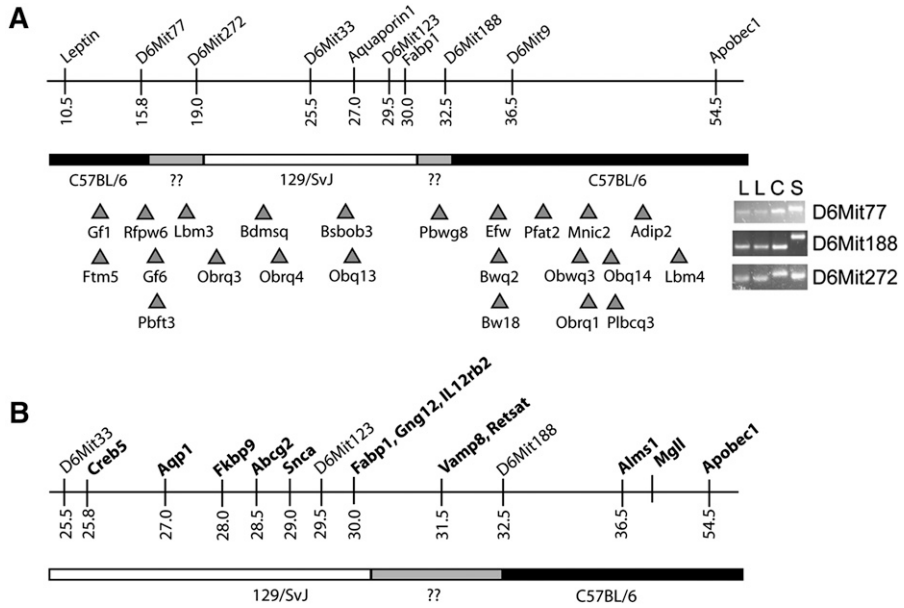

Fig. 3. Obesity-related QTL and genes near *Fabp1* locus. A: Upper portion shows a schematic diagram of genes and markers near *Fabp1*, with genetic background in our *L-Fabp*$^{-/-}$ mice (determined using strain-specific SSLP markers) shown below. Regions confirmed to be C57BL/6J gDNA are black, regions of 129/SvJ gDNA are white, and undetermined areas are gray. Triangles depict the approximate location of QTLs related to body weight and obesity near *Fabp1* gene based on peak association. QTL shown are: Gf1, gonadal fat weight 1; Ftm5, fat tissue mass 5; Rfpw6, retroperitoneal fat pad weight 6; Gf6, gonadal fat weight 6; Pbft3, percent body fat 3; Lbm3, lean body mass 3; Obrq3, obesity resistance QTL 3; Bdmsq, body mass QTL; Obrq4, obesity resistance QTL 4; Bsbob3, BSB obesity 3; Obq13, obesity QTL 13; Pbwg8, postnatal body weight growth 8; Efw, epididymal fat weight; Bwq2, body weight QTL 2; Bw18, body weight 18; Pfat2, predicted fat percentage 2; Obwq3, obesity and body weight QTL 3; Mnic2, macronutrient intake, carbohydrate 2; Obrq1, obesity resistance QTL 1; Obq14, obesity QTL 14; Plbcq3, pleiotropic body composition QTL 3; Adip2, adiposity 2; Lbm4, lean body mass 4. The inset on the right shows PCR products from reactions using three informative SSLP markers. Letters indicate gDNA template for each reaction: L, *L-Fabp*$^{-/-}$; C, C57BL/6J; S, 129/SvJ. B: Expanded view of region surrounding *Fabp1* gene showing position of genes examined for differences in expression between C57BL/6J and *L-Fabp*$^{-/-}$ mice (Table 2).

DISCUSSION

In the current study, we show that aged *L-Fabp*$^{-/-}$ mice fed a low-fat chow diet exhibit reduced body weight and adiposity and attenuated hepatic steatosis compared with WT mice, with differences apparent after 20 weeks. These findings parallel our previous observation that female C57BL/6J congenic *L-Fabp*$^{-/-}$ mice fed a variety of high-SF diets exhibit reduced obesity and hepatic steatosis (15, 17), a phenotype we attributed to a subtle change in consumption of a high-fat diet. The current studies extend those observations by demonstrating alterations in acute feeding behavior in both chow- and SF-fed *L-Fabp*$^{-/-}$ mice. These changes in feeding behavior correlate with altered

TABLE 2. Expression of structural genes near *Fabp1* locus on chromosome 6

Gene	cM	Genomic Location	Young Mice		Aged Mice	
			C57BL/6J	*L-Fabp*$^{2/2}$	C57BL/6J	*L-Fabp*$^{2/2}$
Creb5	25.8	53523368-53645826 (+)	1.03 ± 0.13	0.88 ± 0.17	1.01 ± 0.08	0.68 ± 0.10[a]
Aqp1	27.0	55286426-55298549 (+)	1.01 ± 0.05	0.96 ± 0.04	1.09 ± 0.26	0.73 ± 0.19
Fkbp9	28.0	56782053-56829352 (+)	1.00 ± 0.04	1.32 ± 0.09[a]	1.02 ± 0.13	1.24 ± 0.18
Abcg2	28.5	58534517-58642863 (+)	1.01 ± 0.05	1.30 ± 0.06[a]	1.05 ± 0.19	1.27 ± 0.08
Gng12	30.0	66846391-66971344 (+)	1.00 ± 0.02	1.03 ± 0.03	1.07 ± 0.23	0.85 ± 0.13
Il12rb2	30.1	67241312-67326182 (−)	1.02 ± 0.09	1.25 ± 0.08	1.16 ± 0.34	0.67 ± 0.14
Fabp1, exon 1/2	30.0	71149821-71155017 (+)	1.02 ± 0.10	0.0005 ± 0.0004[b]	1.03 ± 0.16	0.0004 ± 0.0004[b]
Fabp1, exon 3/4	30.0	71149821-71155017 (+)	1.05 ± 0.16	0.0006 ± 0.0003[b]	1.02 ± 0.13	0.0008 ± 0.0003[b]
Vamp8	31.5	72335217-72340697 (−)	1.01 ± 0.06	1.11 ± 0.05	1.02 ± 0.10	0.86 ± 0.05
Retsat	32.3	72548469-72558408 (+)	1.11 ± 0.23	1.15 ± 0.17	1.05 ± 0.18	0.47 ± 0.08[a]
Alms1	36.5	85537525-85652747 (+)	1.00 ± 0.04	1.12 ± 0.11	1.02 ± 0.13	0.84 ± 0.12
Mgll	39.5	88674406-88778354 (+)	1.02 ± 0.10	1.18 ± 0.05	1.03 ± 0.14	0.67 ± 0.05
Apobec1	54.5	122527810-122552462 (−)	1.03 ± 0.12	1.13 ± 0.05	1.04 ± 0.15	0.95 ± 0.09

Gene expression was surveyed in livers of young (3-month-old) or aged (13-month-old) C57BL/6J female mice. n = 4–5 animals per group.
[a] $P < 0.05$.
[b] $P < 0.01$.

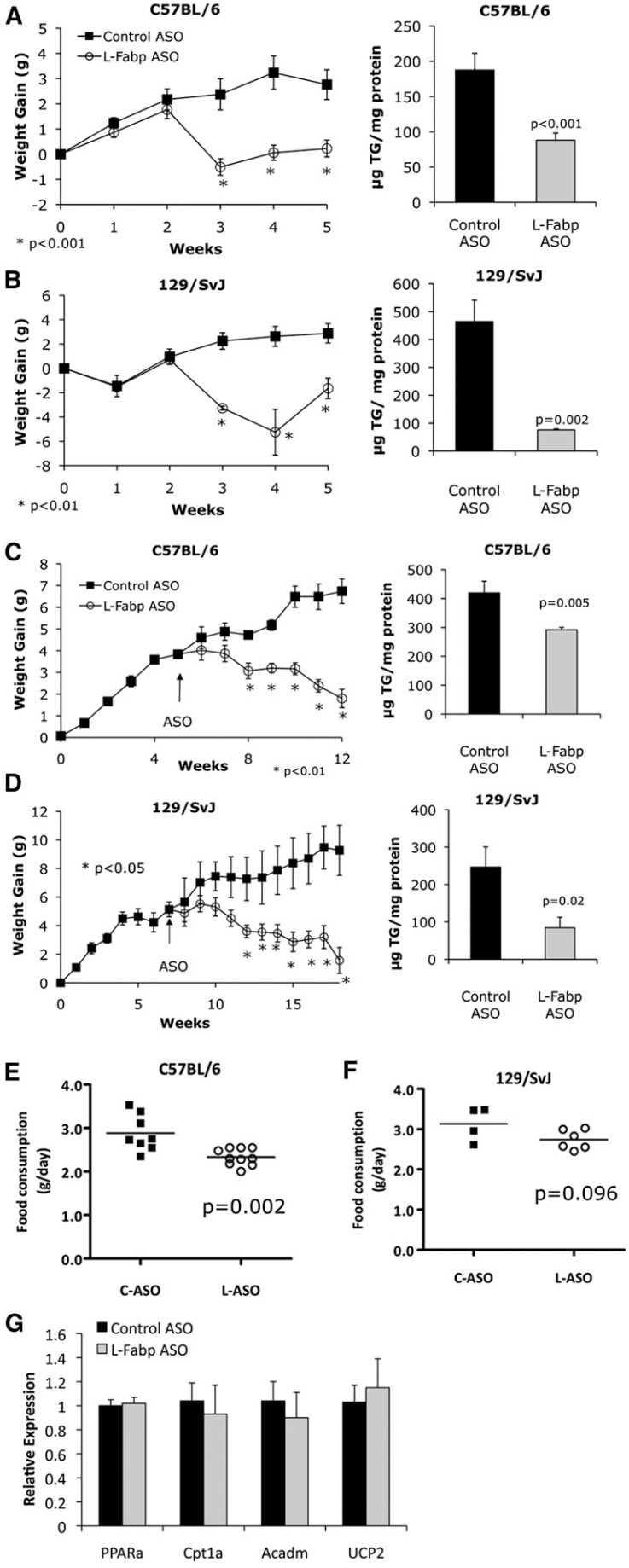

Fig. 4. Liver-specific knockdown of *L-Fabp* reduces diet-induced obesity. A, B: *L-Fabp* ASO prevents diet-induced obesity (left panels) and hepatic steatosis (right panels). C57BL/6J (A) and 129/SvJ (B) mice were started on a Western diet concomitant with start of control (C-ASO, black squares) or *L-Fabp*–specific ASO (L-ASO, open circles) injection. Right panels: Hepatic TG content in ASO-treated mice. For C57BL/6J mice, n = 8 C-ASO, n = 12 L-ASO; for 129/SvJ mice, n = 4 C-ASO, n = 4 L-ASO. C, D: Treatment with *L-Fabp* ASO reverses diet-induced obesity and hepatic steatosis. C57BL/6J (C) and 129/SvJ (D) mice were fed a high-SF diet for 5–7 weeks prior to start of ASO treatment. Right panels show hepatic TG content in ASO-treated mice. For C57BL/6J mice, n = 8 C-ASO, n = 10 L-ASO for body weight and n = 4 C-ASO, n = 6 L-ASO for hepatic lipid. For 129/SvJ mice, n = 4 C-ASO, n = 6 L-ASO for both panels. $*P < 0.05$ compared with C-ASO mice. E, F: Average daily food consumption measured over 2 days in ASO-treated C57BL/6J (E) and 129/SvJ (F) mice fed a high-SF diet, measured ~4 weeks after start of ASO injections. G: Expression of fatty acid oxidation genes in livers of ASO-treated C57BL/6J mice fed Western diet. n = 4 animals/group.

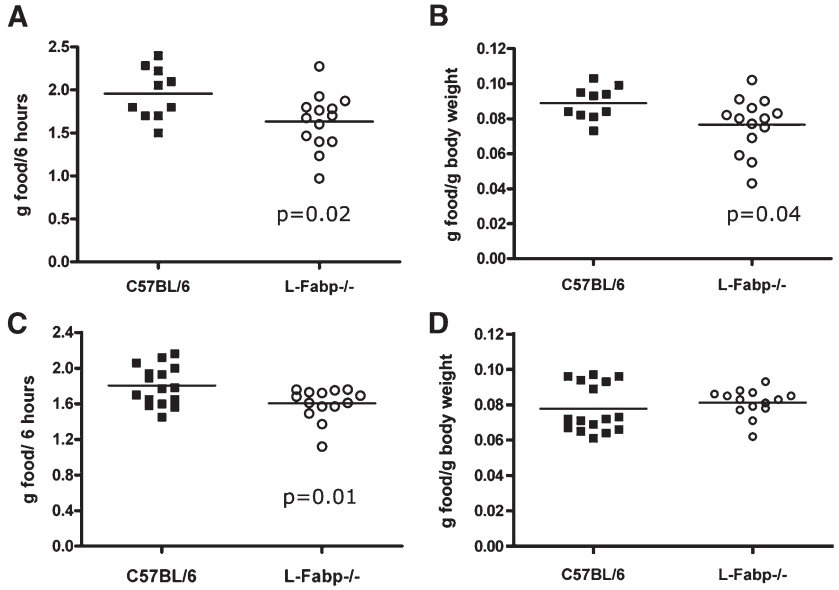

Fig. 5. Altered acute food consumption in *L-Fabp*$^{-/-}$ mice. A, B: Acute food consumption in C57BL/6J and *L-Fabp*$^{-/-}$ mice fed a chow diet, presented either as grams consumed per 6 h (A) or normalized to body weight (B). n = 10–15 mice/genotype. C, D: Acute food consumption in C57BL/6J and *L-Fabp*$^{-/-}$ mice fed a high-SF diet, presented either as grams consumed per 6 h (C) or normalized to body weight (D). Average body weight at time of experiment: C57BL/6J mice, 23.5 ± 0.6 g; *L-Fabp*$^{-/-}$ mice, 19.8 ± 0.4 g; $P < 0.001$. n = 14–16 mice/genotype.

hepatic levels of key lipid mediators of feeding behavior, including AEA and OEA, in *L-Fabp*$^{-/-}$ mice. We postulate that changes in FAE metabolism contribute to altered acute feeding behavior and may explain the protection against obesity and hepatic steatosis in *L-Fabp*$^{-/-}$ mice, perhaps via augmented hepatic AEA hydrolysis resulting in attenuated orexigenic drive. Several elements of these findings merit further discussion.

As mentioned above, an independently generated line of *L-Fabp*$^{-/-}$ mice exhibit a very different phenotype, with increased adiposity and body weight in chow-fed mice at six months of age, and in younger mice fed a high-cholesterol diet (19, 27). In earlier studies, we were unable to replicate that obese phenotype in female *L-Fabp*$^{-/-}$ mice fed a high-cholesterol diet (15), and our current findings again failed to replicate an obese phenotype in chow-fed, aged *L-Fabp*$^{-/-}$ mice. In our search to explain how deletion of the same gene could produce a nearly opposite phenotype in two different laboratories, we surveyed expression of genes near the *Fabp1* locus and surrounding obesity-related QTLs, including some genes (*Alms1, Retstat, Aqp1*) that have been implicated in metabolic adaptations and body weight maintenance (28–33). No evidence was found for gene duplication or altered expression of modifier genes in this region in our *L-Fabp*$^{-/-}$ mice. We attempted to mitigate the potential influence of genetic background in this phenotype by using ASO-mediated knockdown of hepatic *L-Fabp* in both C57BL/6J and 129/SvJ mice. Importantly, knockdown of *L-Fabp* both prevented and reversed diet-induced obesity and hepatic steatosis in each of these inbred strains, recapitulating the phenotypes we observed previously in germline *L-Fabp*$^{-/-}$ mice in a congenic C57BL/6J background (15, 17). The current findings strongly suggest that, in our hands, the effect of *L-Fabp* deletion on body weight and hepatic steatosis is independent of genetic background. It remains unclear how germline deletion of the same gene resulted in such a discrepant phenotype, but we suspect that replication of these studies with both lines of mice in parallel may provide clarification. These studies are currently underway.

Despite the relatively dramatic phenotype of *L-Fabp*$^{-/-}$ mice, the mechanism(s) responsible for obesity protection is remarkably subtle. Despite a decrease in intestinal cholesterol absorption (Fig. 1E) and altered kinetics of mucosal triglyceride mobilization (17), there is no overall defect in dietary fat absorption. In addition, we find no evidence for increased hepatic utilization of FA via oxidation or energy expenditure in *L-Fabp*$^{-/-}$ mice (Ref. 17 and Figs. 1F and 4G), essentially ruling these out as possible mechanisms for protection against age-dependent obesity. We have shown that *L-Fabp*$^{-/-}$ mice exhibit a subtle, but nonsignificant, trend toward decreased food consumption when fed a high-SF diet (15), and that treatment with L-Fabp ASO reduced average daily food consumption compared with C57BL/6J mice treated with control ASO. Acute food consumption studies demonstrated that *L-Fabp*$^{-/-}$ mice consistently consume less food than C57BL/6J mice after fasting/refeeding. However, in the setting of hyperphagia (*Ob/Ob* leptin-deficient), differences in body weight between *L-Fabp*–deficient (*L-Fabp*$^{-/-}$ *Ob/Ob*) and *L-Fabp*–sufficient (*Ob/Ob*) animals were abrogated, indicating that differences in food consumption may play a key role in the attenuated body weight gain and hepatic steatosis in aging *L-Fabp*$^{-/-}$ mice. That said, an unexplained feature of our work is that the average daily food consumption was unchanged between the genotypes of the aged mice and, if

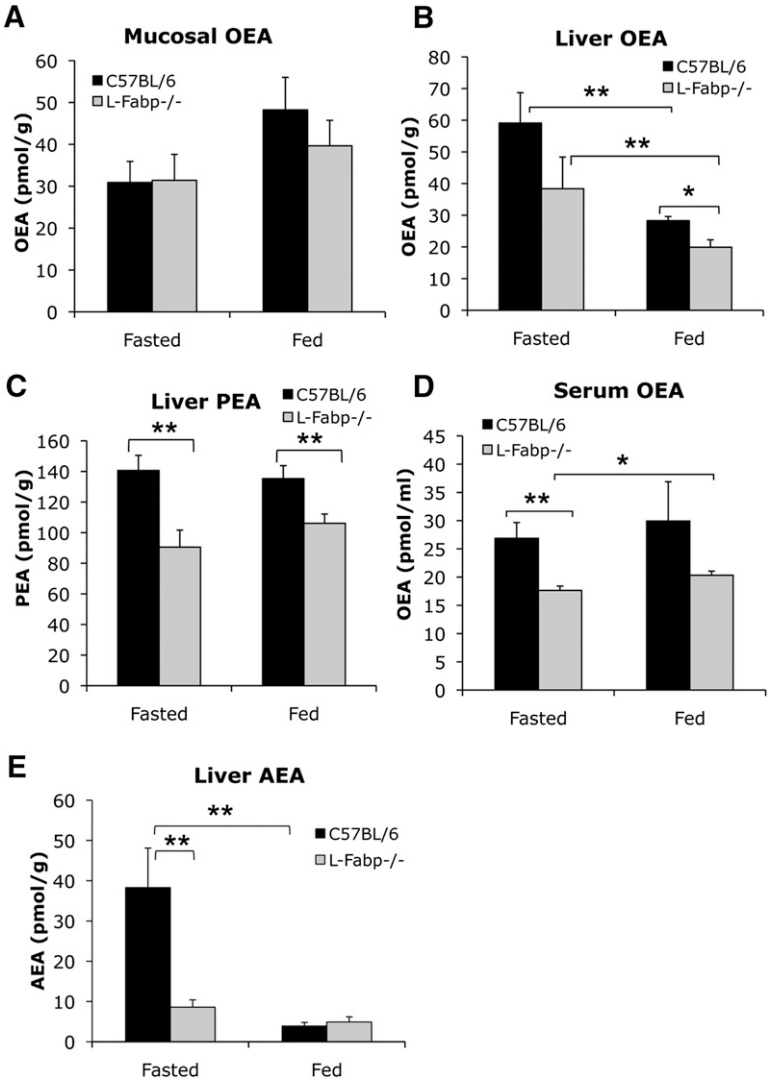

Fig. 6. Fatty acid ethanolamide levels in fasting and fed C57BL/6J and *L-Fabp*$^{-/-}$ mice. OEA content in jejunal mucosa (A), liver (B), and serum (D) of free-fed and fasted mice. n = 5–10 mice/genotype and treatment group. Hepatic levels of the satiety-promoting fatty acid amide PEA (C) and the orexigenic amide AEA (E) were also measured in both free-fed and fasted mice. n = 5–10 animals/genotype and treatment group. For all panels, *$P < 0.05$, **$P < 0.02$.

anything, tended to be higher in the *L-Fabp*$^{-/-}$ mice. It is worth noting, however, that average daily food intake measurements reflect only a snapshot in time and may not discern real differences, and it has been suggested that even with the most sensitive techniques, differences of ±10% cannot be reliably detected (24). It possible that changes in acute feeding behavior (e.g., the quantity of food consumed per hour after fasting and the meal latency) may alter energy utilization (25, 34), as implied by our earlier findings of increased respiratory exchange ratios in *L-Fabp*$^{-/-}$ mice (17).

On the basis of these findings and our previous observations that the kinetics of intestinal and hepatic FA trafficking are altered in *L-Fabp*$^{-/-}$ mice (17), we postulated that altered production or signaling of lipid-derived anorectic or orexigenic factors might correlate with altered feeding behavior. Prior studies demonstrated a role for intestinal OEA production in linking dietary fat intake to satiety (4). We found a comparable increase in intestinal OEA abundance from the fasted to the fed state in both genotypes, but we found a divergence in hepatic OEA abundance (decreased in *L-Fabp*$^{-/-}$ mice), particularly in the fed state. We further demonstrated that levels of the orexigenic amide AEA were markedly reduced in livers of fasted *L-Fabp*$^{-/-}$ mice, with levels similar to those found in fed mice (Fig. 6E). We postulate that alterations in hepatic lipid amide abundance, specifically, reduced hepatic abundance of AEA, may be associated with the altered feeding behaviors noted in *L-Fabp*$^{-/-}$ mice. *FAAH1*$^{-/-}$ mice demonstrate increased endogenous levels of both AEA and OEA in liver, intestine, and hypothalamus, yet they display increased body weight and adiposity and differences in high-fat food consumption (35). Those data point to a hierarchy between AEA and OEA, with elevated AEA levels promoting food consumption and energy storage, overriding the anorectic effects of elevated OEA. In the livers of *L-Fabp*$^{-/-}$ mice, we observed the opposite scenario (i.e., reduced levels of both OEA and AEA), yet a similar hierarchy with the net result (decreased short-term food consumption) correlating with reduced AEA levels. It is worth noting that while ASO-mediated knockdown produced a similar obesity-protection phenotype as the germline *L-Fabp* knockout (including decreased food consumption), we did not observe dramatic alterations in baseline FAE levels in livers of chow-fed L-ASO–treated mice compared with control ASO mice (data not shown).

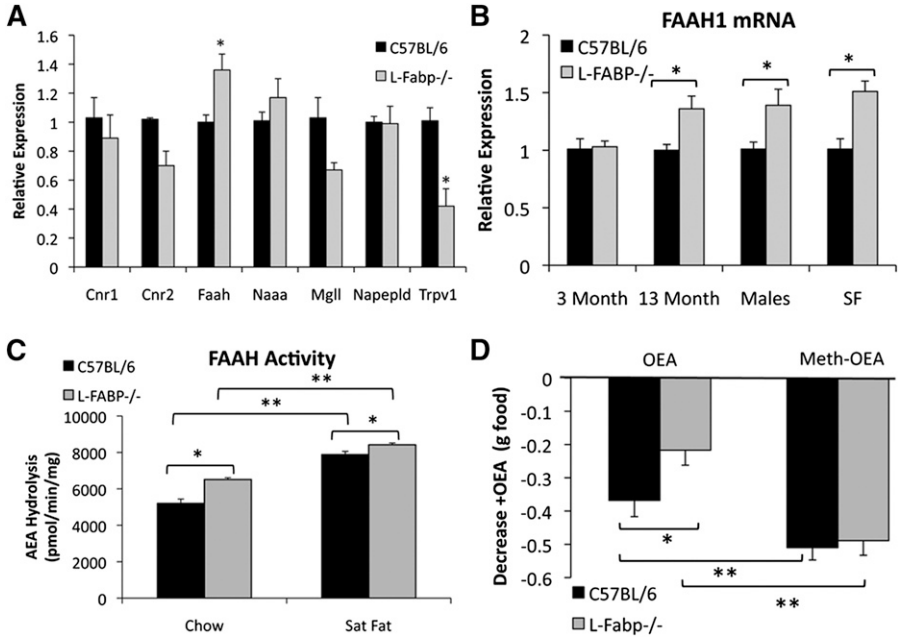

Fig. 7. Increased FAAH expression and activity in livers of *L-Fabp*$^{-/-}$ mice correlates with altered responsiveness to OEA. A: Expression of genes related to fatty acid amide synthesis, signaling, and metabolism in livers of aged chow-fed female C57BL/6J and *L-Fabp*$^{-/-}$ mice. Cnr1, cannabinoid receptor 1; Cnr2, cannabinoid receptor 2; Faah1, fatty acid amide hydrolase; Naaa, n-acylethanolamine acid amidase; Mgll, monoglyceride lipase; Napepld, n-acyl phosphatidylethanolamine phospholipase D; Trpv1, transient receptor potential cation channel v1. *$P < 0.05$ versus C57BL/6; n = 4–5 animals/genotype. B: FAAH-1 mRNA in livers of WT and *L-Fabp*$^{-/-}$ mice. Males are ~1-year-old chow-fed mice. SF are ~26-week-old female mice fed a high-SF diet for 16 weeks. n = 4–5 animals/group. C: FAAH activity in liver membranes of chow-fed and SF diet-fed mice. n = 4–5 mice/group. D: *L-Fabp*$^{-/-}$ mice exhibit blunted response to OEA (left bars) but not to the nonhydrolyzable OEA analog Meth-OEA (right bars) as shown by food consumed in 2 h following agonist injection. Data are presented as average decrease in food consumption in OEA/Meth-OEA–injected mice versus baseline. For Meth-OEA, n = 7–9 mice per genotype; for OEA, n = 11–13 mice per genotype. For all panels, *$P < 0.05$, **$P < 0.01$.

The explanation for this is not clear, but we did not systematically evaluate changes in fed versus fasted hepatic FAE levels or serum FAE levels, and we cannot exclude short-term compensatory changes in other pathways.

Our findings imply that the liver may play a role in regulating systemic levels of AEA and other signaling lipid amides. We observed, consistent with this implication, increased abundance and activity of FAAH in livers of older and high-fat–fed *L-Fabp*$^{-/-}$ mice that correlated with both the decrease in hepatic FAE levels and with decreased responsiveness to exogenous OEA. In vivo studies using the FAAH-insensitive OEA analog Meth-OEA demonstrated that the attenuated response to OEA in *L-Fabp*$^{-/-}$ mice is likely due to increased FAAH activity, as injection of Meth-OEA produced a striking decrease in food consumption in both genotypes. The mechanism by which hepatic FAAH expression and activity is increased in *L-Fabp*$^{-/-}$ mice is not immediately apparent and will be a focus of future investigation.

The decreased responsiveness to OEA in *L-Fabp*$^{-/-}$ mice may also reflect alterations in intracellular trafficking. Recent studies showed that overexpression of FABP7 and FABP5 increased uptake and hydrolysis of AEA in Cos7 cells, suggesting that FABPs may facilitate the intracellular trafficking of this hydrophobic ligand (13). It is tempting to speculate that L-Fabp may play a role in facilitating intracellular movement of either fatty acids for FAE synthesis and/or OEA/AEA for FAAH-mediated degradation, any of which could conceivably result in altered FAE metabolism in *L-Fabp*$^{-/-}$ animals, particularly in response to feeding. Further studies will address these possibilities. The current findings support the suggestion (13) that cell-specific alterations in FAE trafficking and metabolic inactivation play an important role in maintaining tone of lipid-activated PPARα and cannabinoid receptors.

The authors acknowledge the assistance of Trey Coleman in the NORC (DK-56341) for help with the DEXA and MRI studies and Ana Guijarro Anton for discussion. The contribution of the Agilent Technologies/UCI Analytical Discovery Facility, Center for Drug Discovery is gratefully acknowledged.

REFERENCES

1. Foster-Schubert, K. E., and D. E. Cummings. 2006. Emerging therapeutic strategies for obesity. *Endocr. Rev.* **27:** 779–793.
2. Cao, H., K. Gerhold, J. R. Mayers, M. M. Wiest, S. M. Watkins, and G. S. Hotamisligil. 2008. Identification of a lipokine, a lipid hormone linking adipose tissue to systemic metabolism. *Cell.* **134:** 933–944.
3. Gillum, M. P., D. Zhang, X. M. Zhang, D. M. Erion, R. A. Jamison, C. Choi, J. Dong, M. Shanabrough, H. R. Duenas, D. W. Frederick, et al. 2008. N-acylphosphatidylethanolamine, a gut- derived circulating factor induced by fat ingestion, inhibits food intake. *Cell.* **135:** 813–824.

4. Schwartz, G. J., J. Fu, G. Astarita, X. Li, S. Gaetani, P. Campolongo, V. Cuomo, and D. Piomelli. 2008. The lipid messenger OEA links dietary fat intake to satiety. *Cell Metab.* **8:** 281–288.
5. Fu, J., S. Gaetani, F. Oveisi, J. Lo Verme, A. Serrano, F. Rodriguez De Fonseca, A. Rosengarth, H. Luecke, B. Di Giacomo, G. Tarzia, et al. 2003. Oleylethanolamide regulates feeding and body weight through activation of the nuclear receptor PPAR-alpha. *Nature.* **425:** 90–93.
6. Capasso, R., and A. A. Izzo. 2008. Gastrointestinal regulation of food intake: general aspects and focus on anandamide and oleoylethanolamide. *J. Neuroendocrinol.* **20(Suppl. 1):** 39–46.
7. Hansen, H. S., and T. A. Diep. 2009. N-acylethanolamines, anandamide and food intake. *Biochem. Pharmacol.* **78:** 553–560.
8. Fu, J., G. Astarita, S. Gaetani, J. Kim, B. F. Cravatt, K. Mackie, and D. Piomelli. 2007. Food intake regulates oleoylethanolamide formation and degradation in the proximal small intestine. *J. Biol. Chem.* **282:** 1518–1528.
9. Fu, J., J. Kim, F. Oveisi, G. Astarita, and D. Piomelli. 2008. Targeted enhancement of oleoylethanolamide production in proximal small intestine induces across-meal satiety in rats. *Am. J. Physiol. Regul. Integr. Comp. Physiol.* **295:** R45–R50.
10. Fu, J., F. Oveisi, S. Gaetani, E. Lin, and D. Piomelli. 2005. Oleoylethanolamide, an endogenous PPAR-alpha agonist, lowers body weight and hyperlipidemia in obese rats. *Neuropharmacology.* **48:** 1147–1153.
11. Osei-Hyiaman, D., M. DePetrillo, P. Pacher, J. Liu, S. Radaeva, S. Batkai, J. Harvey-White, K. Mackie, L. Offertaler, L. Wang, et al. 2005. Endocannabinoid activation at hepatic CB1 receptors stimulates fatty acid synthesis and contributes to diet-induced obesity. *J. Clin. Invest.* **115:** 1298–1305.
12. Siegmund, S. V., E. Seki, Y. Osawa, H. Uchinami, B. F. Cravatt, and R. F. Schwabe. 2006. Fatty acid amide hydrolase determines anandamide-induced cell death in the liver. *J. Biol. Chem.* **281:** 10431–10438.
13. Kaczocha, M., S. T. Glaser, and D. G. Deutsch. 2009. Identification of intracellular carriers for the endocannabinoid anandamide. *Proc. Natl. Acad. Sci. USA.* **106:** 6375–6380.
14. Storch, J., and A. E. Thumser. 2010. Tissue-specific functions in the fatty acid-binding protein family. *J. Biol. Chem.* **285:** 32679–32683.
15. Newberry, E. P., S. M. Kennedy, Y. Xie, B. T. Sternard, J. Luo, and N. O. Davidson. 2008. Diet-induced obesity and hepatic steatosis in L-Fabp-/- mice is abrogated with SF, but not PUFA, feeding and attenuated after cholesterol supplementation. *Am. J. Physiol. Gastrointest. Liver Physiol.* **294:** G307–G314.
16. Newberry, E. P., Y. Xie, S. Kennedy, X. Han, K. K. Buhman, J. Luo, R. W. Gross, and N. O. Davidson. 2003. Decreased hepatic triglyceride accumulation and altered fatty acid uptake in mice with deletion of the liver fatty acid-binding protein gene. *J. Biol. Chem.* **278:** 51664–51672.
17. Newberry, E. P., Y. Xie, S. M. Kennedy, J. Luo, and N. O. Davidson. 2006. Protection against Western diet-induced obesity and hepatic steatosis in liver fatty acid-binding protein knockout mice. *Hepatology.* **44:** 1191–1205.
18. Lagakos, W. S., A. M. Gajda, L. Agellon, B. Binas, V. Choi, B. Mandap, T. Russnak, Y. X. Zhou, and J. Storch. 2011. Different functions of intestinal and liver-type fatty acid-binding proteins in intestine and in whole body energy homeostasis. *Am. J. Physiol. Gastrointest. Liver Physiol.* **300:** G803–G814.
19. Martin, G. G., B. P. Atshaves, A. L. McIntosh, J. T. Mackie, A. B. Kier, and F. Schroeder. 2008. Liver fatty acid-binding protein gene-ablated female mice exhibit increased age-dependent obesity. *J. Nutr.* **138:** 1859–1865.
20. Newberry, E. P., S. M. Kennedy, Y. Xie, J. Luo, and N. O. Davidson. 2009. Diet-induced alterations in intestinal and extrahepatic lipid metabolism in liver fatty acid binding protein knockout mice. *Mol. Cell. Biochem.* **326:** 79–86.
21. Millar, J. S., D. A. Cromley, M. G. McCoy, D. J. Rader, and J. T. Billheimer. 2005. Determining hepatic triglyceride production in mice: comparison of poloxamer 407 with Triton WR-1339. *J. Lipid Res.* **46:** 2023–2028.
22. Astarita, G., B. Di Giacomo, S. Gaetani, F. Oveisi, T. R. Compton, S. Rivara, G. Tarzia, M. Mor, and D. Piomelli. 2006. Pharmacological characterization of hydrolysis-resistant analogs of oleoylethanolamide with potent anorexiant properties. *J. Pharmacol. Exp. Ther.* **318:** 563–570.
23. Newberry, E. P., S. M. Kennedy, Y. Xie, J. Luo, S. E. Stanley, C. F. Semenkovich, R. M. Crooke, M. J. Graham, and N. O. Davidson. 2008. Altered hepatic triglyceride content after partial hepatectomy without impaired liver regeneration in multiple murine genetic models. *Hepatology.* **48:** 1097–1105.
24. Ellacott, K. L., G. J. Morton, S. C. Woods, P. Tso, and M. W. Schwartz. 2010. Assessment of feeding behavior in laboratory mice. *Cell Metab.* **12:** 10–17.
25. Galarce, E. M., and P. C. Holland. 2009. Effects of cues associated with meal interruption on feeding behavior. *Appetite.* **52:** 693–702.
26. Motter, A. L., and G. P. Ahern. 2008. TRPV1-null mice are protected from diet-induced obesity. *FEBS Lett.* **582:** 2257–2262.
27. Atshaves, B. P., A. L. McIntosh, S. M. Storey, K. K. Landrock, A. B. Kier, and F. Schroeder. 2010. High dietary fat exacerbates weight gain and obesity in female liver fatty acid binding protein gene-ablated mice. *Lipids.* **45:** 97–110.
28. Arsov, T., C. Z. Larter, C. J. Nolan, N. Petrovsky, C. C. Goodnow, N. C. Teoh, M. M. Yeh, and G. C. Farrell. 2006. Adaptive failure to high-fat diet characterizes steatohepatitis in Alms1 mutant mice. *Biochem. Biophys. Res. Commun.* **342:** 1152–1159.
29. Arsov, T., D. G. Silva, M. K. O'Bryan, A. Sainsbury, N. J. Lee, C. Kennedy, S. S. Manji, K. Nelms, C. Liu, C. G. Vinuesa, et al. 2006. Fat aussie–a new Alstrom syndrome mouse showing a critical role for ALMS1 in obesity, diabetes, and spermatogenesis. *Mol. Endocrinol.* **20:** 1610–1622.
30. Collin, G. B., E. Cyr, R. Bronson, J. D. Marshall, E. J. Gifford, W. Hicks, S. A. Murray, Q. Y. Zheng, R. S. Smith, P. M. Nishina, et al. 2005. Alms1-disrupted mice recapitulate human Alstrom syndrome. *Hum. Mol. Genet.* **14:** 2323–2333.
31. Moise, A. R., G. P. Lobo, B. Erokwu, D. L. Wilson, D. Peck, S. Alvarez, M. Dominguez, R. Alvarez, C. A. Flask, A. R. de Lera, et al. 2010. Increased adiposity in the retinol saturase-knockout mouse. *FASEB J.* **24:** 1261–1270.
32. Schupp, M., M. I. Lefterova, J. Janke, K. Leitner, A. G. Cristancho, S. E. Mullican, M. Qatanani, N. Szwergold, D. J. Steger, J. C. Curtin, et al. 2009. Retinol saturase promotes adipogenesis and is downregulated in obesity. *Proc. Natl. Acad. Sci. USA.* **106:** 1105–1110.
33. Verkman, A. S. 2009. Knock-out models reveal new aquaporin functions. *Handb. Exp. Pharmacol.* **2009:** 359–381.
34. Duffy, P. H., R. J. Feuers, and R. W. Hart. 1990. Effect of chronic caloric restriction on the circadian regulation of physiological and behavioral variables in old male B6C3F1 mice. *Chronobiol. Int.* **7:** 291–303.
35. Touriño, C., F. Oveisi, J. Lockney, D. Piomelli, and R. Maldonado. 2010. FAAH deficiency promotes energy storage and enhances the motivation for food. *Int. J. Obes. (Lond.).* **34:** 557–568.